Assessment of the antibacterial efficacy of nickel/manganese nanoparticles against staphylococcus aureus

Sarab Murad Alqazaaly [1*] and *Laith* A. Yaaqoob [2]

[1]College of Dentistry, Al-Iraqia University, Baghdad, Iraq
[2]Department of Biotechnology, College of Science, University of Baghdad, Iraq

Abstract. Nickel/Manganese nanoparticles were assessed as an antibacterial agent in the current investigation. Atomic force microscopy and absorption spectroscopy means were used for scanning electron microscopy and Fourier-transform infrared spectroscopy analysis. The nickel/manganese oxide nanoparticles were created by using leaf extract from Lepidium sativum. These nanoparticles were ultimately described using diffraction patterns of X-rays. Two different concentrations were created from the synthesized Nickel/Manganese nanoparticles, and their potential antibacterial action towards *Staphylococcus aureus* was examined. The test results showed that the nanoparticles are spherical, either by themselves or grouped together, and solid for Nickel/Manganese. Their average size is 45.9 nm. Nickel/Manganese nanoparticles restrict bacterial proliferation, as demonstrated by extensive inhibition zones against S. aureus across all tested doses. Moreover, the minimum inhibitory concentration values of Nickel/Manganese nanoparticles against S. aureus isolates No. 2, 5, 6, 7, and 10 were (1 mg/ml), while isolates No. 1, 3, 8, and 9 exhibited minimum inhibitory concentration values of (2 mg/ml), and isolate No. 4 demonstrated a minimum inhibitory concentration of 4 mg/ml. The action against biofilms of Nickel/Manganese nanoparticles in opposition to S. aureus isolates shown inhibition of 80% at (0.5 $mg.ml^{-1}$), 100% at (1 $mg.ml^{-1}$) in biofilm formation.

1 Introduction

There are many pathogenic microorganisms in the environment. They are easily transmitted, have a high potential for negative responses, long-lasting health impacts, and even fatalities. An immediate hazard to people is infection resulting from pathogen invasion into the body, this may develop to illnesses include gastritis ,pneumonia, and sepsis, which may cause harm to tissues cause a malfunctioning organ, and result in mortality[1].
The antibiotics are highly helpful in treating various ailments. The extensive emergence Among bacteria that are multidrug resistant (MDR), which notably diminish the process of

* Corresponding author: Sarab.murad1980@aliraqia.edu.iq

healing effectiveness of medications, is attributable to bacteria employing mutations to improve their resistance to medicines.

Since bacteria tenaciously persevere in developing adaptable defenses against conventional antibiotics, there is growing worry about the development of antibiotic resistance [2]. Infectious illnesses brought on by MDR bacteria and their prevalence, particularly Staphylococcus aureus and multi-antibiotic-resistant bacteria, have risen alarmingly [3].

Creating new antibiotics is a labor-intensive and expensive procedure that takes a long time. Thus, it is therefore highly recommended that new, unusual methods of treating infectious illnesses be developed [4]. This method of nanoparticle manufacturing offers advantages more than physical and chemical approaches since it provides no environmental danger; hence, it may be employed for the biomedical applications [5].

Nanostructured materials have been used on the basis of their efficacy and robustness. These compounds are widely applied in a great variety of fields such as biological, pharmaceutical and physical engineering, environmental and chemical sciences, because of their increased area of surface to volume ratio that they possess [6].

A metal and an oxide of metal nanoparticles are categorized as(mono-, bi-, tri-, or Quadro metallic) according to the quantity of metals current. Bi-, tri-, and Mult metallic nanoparticles have garnered significant attention on account of the heightened catalytic activities and favorable qualities that they possess relative to monometallic nanoparticles [8]. Two separate varieties of metallic atoms are amalgamated to form bimetallic nanoparticles, A unique nanometric substance with a variety of topologies, morphologies, and characteristics [9]. Because of tensile tension and metal synergism, NPs made of bimetallic oxides, such as NiO/MnO, MgO/ZnO, and Fe_3O_4/ZnO NPs, frequently demonstrate distinctive antibacterial efficacy [8]. As a result, as compared to their bulk counterparts, the unique features of nanoparticles create a favourable environment for antibacterial therapy. Several inorganic and organic nanocomposites have antibacterial characteristics that can detect germs quickly and accurately. Antibacterial nanocomposites are designed with specific environmental flexibility and combinatorial delivery methods. [10]. This research aims to assess the antibacterial efficacy of green produced nanoparticles (Ni/Mn-NPs) against Staphylococcus aureus.

2 Materials and methods

It was necessary to clean the leaves of the flora and then cut them into small pieces. 25 g of Lepidium sativum there was a mixture of 100 milliliters of filtered water and leaves, as well as subjected to boiling for 2 h at 90 °C. This was the extract subsequently acquired (Whatmann filter paper) was utilized, and the filtrate was stored for the subsequent procedures [11].

2.1 Synthesis and characterization of nickel/manganese-NPs

All of the materials that is, reagents utilized in the production of Ni/Mn-NPs were procured from Sigma, Ltd, UAS. The preparation involved combining Ni/Mn-NPs with an aqueous extract of Lepidium sativum. was done by mix 1:1 of $MnSO_4.H_2O$ and $NiSO_4.6H_2O$, An ultrasonication bath was used to disperse 10g of mixing for 30 minutes after it had been dissolved in 250ml of deionized distilled water. Following that, ten milliliters of the plant extract were included. and mixed for 60 minutes in the ultrasonic bath. Finally, until solid black Ni/Mn-NPs were produced, 10 M sodium hydroxide was the solution progressively contributed to the mixture of the reaction. Now that the creation of nanoparticles, the particles were separated using Whatman filter paper before being repeatedly rinsed with water to

eliminate any lingering byproducts. Then, The Ni/Mn-NPs that were synthesized were generated in a variety of concentrations, including 32 and 64 mg/ml variations.

2.2 Characterization Techniques for NPs

Atomic force microscopy, or AFM for short, was used to determine the average crystal size in order to depict the two- and three-dimensional structures of the generated Ni/Mn-NPs. For further characterization of the patterns discovered using field emission microscopy (SEM), scanning electron microscopy was utilized. The structure of the crystals was ascertained using an X-ray diffraction examination. Shimadzu equipment was used for FTIR analysis for researching the functional typization of Ni/Mn-NPs groups which have been taken from extracts of herbs. With application of ground rules, the specimens have been manufactured by stretching on a glass slide. The synthesis of Ni/Mn-NPs has been made at the Biotechnology Department, College of Science, University of Baghdad, and the characterization has been made at the Chemistry Department of the same affiliation.

2.3 Antibacterial Activity

2.3.1 Isolation of bacterial strains

A kind of bacterium called Staphylococcus aureus was found and acquired during this experiment. Between March 2021 and November 2022, 150 randomly selected samples of both sexes, ages 1 to 60, were drawn from 65 male and 85 female patients who had burns and wounds that were infected at various Baghdadi hospitals, such as Medical City Hospital, Al-Kindi Hospital, and Martyr Al-Sadr General Hospital. All of the study's confirmation tests were carried out in the lab prior to the trials, and the VITEK-2 System was used to authenticate the medical diagnosis. The microbes were then stimulated by culture, which involved heating nutritious broth to 37 degrees Celsius for 24 hours in order to assess the efficacy of antibiotics.

2.3.2 Susceptibility to Anti antibiotics

The World Health Organization states that the Kirby-Bauer approach includes the following:
[12, 15], The antibiotic susceptibility of fourteen different drugs was assessed. The bacterial suspension that resulted from separating one or two colonies of bacteria from the original culture and putting them in a test tube with four milliliters of regular saline showed a modest amount of turbidity compared to the standard turbidity solution. The corresponding value is (1.5 × 10^8) CFU/ml. A sterile cotton swab was used to spread and uniformly distribute a quantity of the bacterial solution throughout the Mueller-Hinton agar medium. Then 10 minutes given to settle. The antimicrobial discs were then carefully positioned on the agar using sterile forceps to make sure it was feasible to see them in contact with the agar. Subsequently, the plates were incubated for 18 to 24 hours at 37 degrees Celsius while inverted. The inhibitory zones that surrounded the discs were measured using a metric ruler in accordance with the guidelines given by the Clinical Laboratories Standards Institute, and the measurements were expressed in millimeters (mm) [13].

2.3.3 Evaluation of biofilm

Thus, instructions were given [14], and an evaluation was conducted to determine whether or not S. aureus is capable of quantifying the data generated by biofilms. During the course of the night, each and every isolator was subjected to Stem Cell Infusion. At 37

degrees Celsius, the broth was heated. An introduction was made to a broth that was created with tryptic soy broth (TSB) that was supplemented with 1% glucose and properly homogenized using a pipette. Each isolate was introduced to the broth. For the purpose of the suspension, the ambiguous state of the bacterial isolate McFarland No. 0.5 was utilized volume containing (200 microliters) of the culture of each individual isolate was put in triplicate on a sterile, flat-bottomed 96-well microtiter plate. Twenty-four hours were spent incubating the plate at 37 degrees Celsius in an aerobic atmosphere with covers in place. The temperature was maintained during the whole process. The planktonic cells were discovered to be devoid of bacteria after being rinsed twice with distilled water. This was done in order to eliminate the microorganisms that had been present during the incubation phase. In order to fix the bacterial cells that are sticking in each well for twenty minutes at room temperature, two hundred microliters of methanol that is one hundred percent was utilized. In order to stain the adhering cells, 200 microliters of crystal violet with a concentration of 0.1% were put into each well and allowed to incubate for a duration of 15 minutes. After the staining procedure was finished, any extra stain was removed by washing the item many times with distilled water on two to three separate occasions.
After allowing the plate to air dry at room temperature for about thirty minutes, it is determined that it is completely dry. This is done to confirm that the plate is completely dry. A 33% acetic acid solution is then used to remove the discoloration. An automated ELISA reader operating at 630 nm wavelength is required to analyze the optical density (OD) test results. After calculating the results of everyone's tests, it was decided that the average optical density values of the sterile medium would not be included in the analysis. The cutoff value, also known as ODc, was computed in order to determine whether or not the isolates were biofilm producers or non-producers [15].

ODc: The mean optical density of the negative control plus three times the negative control's standard deviation (SD).

OD isolate: ODc stands for the average optical density of the isolate. The following is the outcome of the biofilm detection that was determined by the computation of the cutoff value (ODc):
OD ≤ ODc There is no creation of biofilm.
ODc < OD ≤ 2 × ODc (the generation of biofilm is poor).
2 × ODc < OD ≤ 4 × ODc (generation of biofilm that is modest).
4× ODc < OD (high levels of biofilm in production).

2.3.4 Antibacterial efficacy of (nickel/manganese NPs) using the Disc diffusion method.

Disc diffusion was the method that was used to identify the existence of antibacterial activity in Ni/Mn-NPs. This method was utilized in accordance with the recommendation made by Razmavar et al. [16]. Antibacterial activity was determined by the utilization of this method. A sterile swab was used to collect the bacterial culture, which was then adjusted to the 0.5 For the purpose of inoculating Mueller-Hinton agar plates in a consistent manner, the McFarland standard was utilized. The plates were used for the sensitivity test after they had been allowed to come to room temperature for fifteen minutes. A stock solution that has been produced using Ni/Mn-NPs at concentrations of 32 and 64 mg/ml. Next, twenty µ·l of A sterile blank disc of 6 millimeters in diameter was used for each dilution that was applied. For the purpose of serving as negative controls, distilled water and DMSO discs were utilized. A comprehensive drying procedure was carried out on every disc before it was positioned on the surface of the Mueller Hinton agar in the laboratory. At a temperature of 37 degrees

Celsius, the plates were maintained in an incubator for a period of time ranging from 18 to 24 hours. The diameter of the inhibition zone that surrounds the discs was measured once the incubation time had come to an end. This was done so that the success of the antibacterial treatment could be evaluated. It was necessary to conduct each of the experiments three times in order to increase the likelihood that they would be successful.

2.3.5 Minimum Inhibitory Concentration (MIC) for nickel/manganese NPs

A 96-well microtiter plate was used to measure the minimum inhibitory concentration (MIC) of manganese and nickel nanoparticles by the broth dilution technique.To obtain concentrations of 0.25, 0.5, 1, 2, 4, 8, 16, and 32 (mg/ml) mg/ml, repeated dilutions of Ni/Mn-NPs were rapidly made on the plate after the Ni/Mn-NP working solution was prepared in broth at a concentration of 64 mg/ml. The wells of the first row A were filled with 200 µl of synthesized Ni/Mn nanoparticles. Only 100 µl of broth was added to each column B-H. Using a micropipette, repeated serial dilutions were methodically made in the columns (rows A to H).

After extracting 100 µl of the initial concentration from row A, the mixture is transferred to the next row containing 100 µl of broth and mixed well. The remaining 100 µl is discarded after this process is repeated until the last row (H). The final volume in each test well containing Ni/Mn-NPs is 100 µl. The lone exception to this rule is the sterility control column, which holds 200 µl of broth. One hundred microlitres of the bacterial inoculum, which contained 1×10^6 CFU/ml, was dispensed into each well except the negative control. For 18 to 20 hours, microtiter plates were incubated at 37°C. Twenty microlitres of resazurin dye were added to each well following the incubation time, and the mixture was then incubated for thirty minutes to see any colorimetric changes. The Ni/Mn-NPs' lowest inhibitory concentrations were visually assessed in broth microdilutions for the resazurin broth test. This was done in order to prevent the two colours from changing from blue to pink [17].

2.3.6 Antibiofilm Activity of (Nickel/Manganese-NPs)

The effectiveness of Ni/Mn-NPs in preventing the formation of biofilm was determined by using a microtiter plate with 96 wells. Ni/Mn-NPs solution was prepared at 32 mg/ml, allowing for a range of concentrations from 32 to 0.25 mg/ml. The starting wells were consisting of the only wells in row A that had 200 µl of each sample. On the other hand, rows B through H contained 100 µl of the broth. Systematic twofold serial dilutions were executed down the columns (from rows A to H) utilizing a micropipette. A total volume of 100 microliters was extracted from the initial concentrations in row A. This volume was then transferred to the adjacent row, which contained 100 microliters of broth, well mixed. Repetition of this technique was carried out until the final row (H), at which point the final 100 µl was discarded. In each well, 100 µl of the bacterial inoculum at a concentration of 1×10^6 CFU/ml was delivered, with the exception of the negative control. The methodology described in the paragraph (Assessment of biofilm formation) was utilized in this study.

2.3.7 Statistical evaluation

The analysis of variance (ANOVA) was conducted in a one-way fashion for this study. The statistical analysis was performed using SPSS version 23, with p values less than 0.01 indicating statistically significant differences. The evaluation of correlations and the significance of differences was carried out. The calculation of the mean was performed by utilising the standard deviation, which was utilised for the purpose of expressing the provided data.

3 Results and Discussion

3.1 Antibiotic Susceptibility

The current investigation's findings showed that every isolate of Staphylococcus aureus exhibited variety. This was because they were resistant to every one of the fourteen drugs that were utilized in this study. Table 1 shows the results of an evaluation of the Staphylococcus aureus isolates' antibiotic sensitivity. A hundred percent of the twenty bacterial isolates showed complete antimicrobial resistance to the medication ceftazidime, vancomycin, and azithromycin. There was a one hundred percent rate of bacterial resistance to the medicines imipenem and cefotaxime. The bacterial isolates shown substantial resistance to antibiotics such as amikacin, trimethoprim, and norfloxacin. These are all examples of antibiotic resistance at percentages of 65%, 55%, and 50%, respectively, in the corresponding cases. Tetracycline, Ciprofloxacin, Trimethoprim/sulfamethoxazole, and Levofloxacin came in second, third, fourth, and fifth, respectively, with 60%, 55%, 55%, and 50% concentrations, respectively, when it came to the relative sensitivity of the bacterial isolates that were examined. Gentamicin and Tobramycin, in particular, exhibited a relative sensitivity of 65% each. Consequently, for the purpose of this investigation, 10 samples of S. aureus that exhibited a high level of antibiotic resistance were selected. The present research findings are very much harmonious with those of many other investigations. For example, we see it here [18] and in many other papers of similar field

Table 1. Number of isolates and proportion of antibiotic-resistant Staphylococcus aureus

Antibiotics	**symbol**	**Resistance**		**Intermediate**		**Sensitive**		**Total %**
		No.	**%**	**No.**	**%**	**No.**	**%**	
Cefotaxime (30µg)	CTX	18	90	0	0	2	10	20(100)
Imipenem (10µg)	IPM	18	90	0	0	2	10	20(100)
Ciprofloxacin (10µg)	CIP	8	40	1	5	11	55	20(100)
Levofloxacin (5µg)	LEV	9	45	1	5	10	50	20(100)
Trimethoprim (10µg)	TM	11	55	1	5	8	40	20(100)
Amikacin(10µg)	AK	13	65	1	5	6	30	20(100)
Vancomycin (10µg)	VA	20	100	0	0	0	0	20(100)
Azithromycin (15 µg)	AZM	20	100	0	0	0	0	20(100)
Tetracycline (10µg)	TE	8	40	0	0	12	60	20(100)
Gentamycin (10µg)	CN	6	30	1	5	13	65	20(100)
Ceftazidime (30µg)	CAZ	20	100	0	0	0	0	20(100)
Norfloxacin (10µg)	NX	10	50	0	0	10	50	20(100)

Trimethoprim/ sulfamethoxazole (25µg)	SXT	8	40	1	5	11	55	20(100)
Tobramycin (10µg	TOB	6	30	1	5	13	65	20(100)

3.2 Detecting Biofilm

Bacteria often use the development of biofilms as a means of survival in hostile environments. In natural aquatic ecosystems as well as on collections of abiotic surfaces frequently used in water systems, bacteria can form biofilms [19]. To measure the strength of the biofilm, the microtiter plate technique was employed for the purpose of determining the quantity of biofilm formation. As indicated in (Table 2), the results demonstrated that all isolates had substantial biofilm development, except for the ninth and tenth isolates.

Table 2. Biofilm forming of *S. aureus* isolates

***S.uareus* Isolate**	**S1**	**S2**	**S3**	**S4**	**S5**	**S6**	**S7**	**S8**	**S9**	**S10**
Biofilm forming	Strong	Strong	Strong	Strong	Strong	Strong	Strong	Strong	Moderate	Moderate

3.3 UV-Visible spectroscopy

When extract of Lepidium sativum was mixed with an aqueous solution of NiO/MnO, the color changed. The observed change was initiated by stimulating the Surface Plasmon Resonance (SPR) vibrations of the metal nanoparticles. The SPR is revealed when a free electron is produced as a result of the interaction between the valence and conduction bands of metal nanoparticles. In the synthesis of Ni/Mn-NPs, a characteristic peak value is produced by the collective oscillation of free metal nanoparticle electrons with light waves resonance. The UV-visible spectra of aqueous plant extracts containing nickel and manganese nanoparticles are shown in Figures 1 and 2. Numerous chemical compounds interact with mineral ions, as seen by the tiny absorption peak at 300 nm [10]. The absorbance associated with surface plasmon resonance is significantly affected by the kind, size, and shape of the generated NPs, temperature, the medium's dielectric constant, and the distances between the particles [11]. UV light can be absorbed by NPs [12]. The UV-visible absorption intensity of nanoparticles frequently increases in proportion to their concentration [8]. The current investigation absorption spectra were obtained from 250 to 1100 nm. Besides, the Ni/Mn-NPs surface plasmon resonance band in the aqueous extract is centered at 367 nm, which is different from utilizing ultraviolet light to analyze aqueous preparations of Lepidium sativum, which measure 270 nm.

.

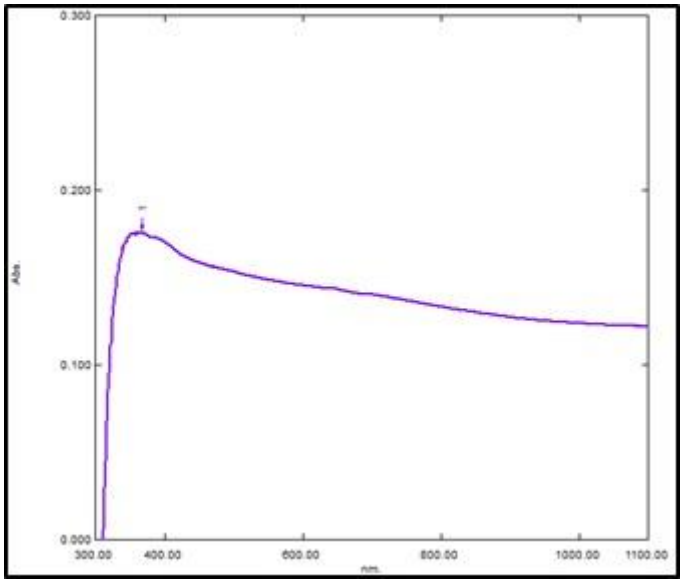

Fig. 1. UV-Visible spectral analysis of *Lepidium sativum* aqueous extracts

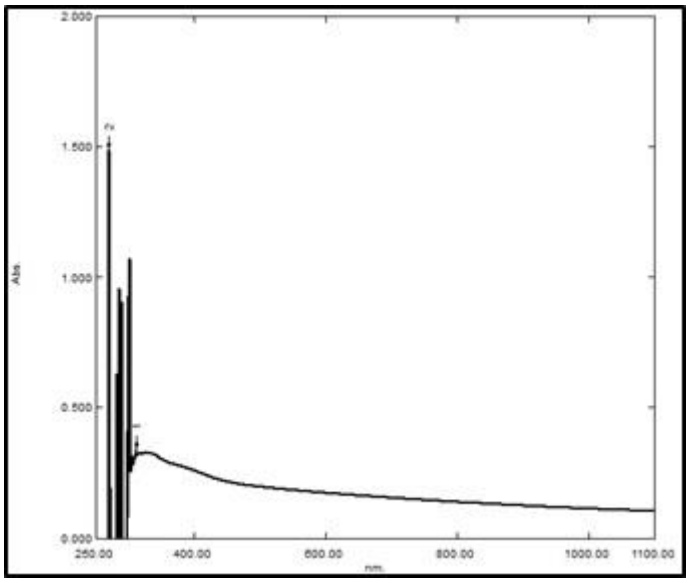

Fig. 2. UV-Visible spectral analysis of Ni/Mn-NPs

3.4 Scanning electron microscope

The shape and form of the green nanoparticles were assessed using methods that are frequently employed to describe synthetic nanoparticles, including the scanning electron microscopy (SEM) technique. The results indicate remarkable variation in nanoparticle morphology, exhibiting a broad array of sizes and shapes. Ni/Mn-NPs' surface has been

examined using a scanning electron microscope (SEM). Ni/Mn-NP particles are spherical and nanoscale in size, based on SEM analysis (Figure 3).

The SEM examination of the Ni/Mn-NPs prepared with *Lepidium sativum* leaf aqueous extract is shown the surface characteristics of the Ni/Mn-NPs sample. The Ni/Mn-NPs are arranged as regular beads in the SEM image, and it is obvious that they are nanometer-sized. The form of the particles is almost spherical, have uniform sizes, and were found to have an average size of about 45.9 nm, which suggests that the green synthesis approach is an effective way to create nickel/manganese oxides (Mix) nanoparticles.

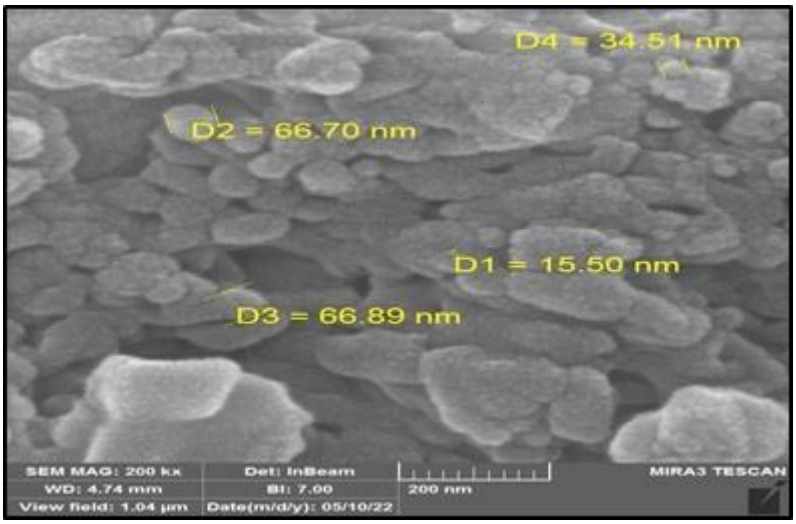

Fig. 3. SEM analysis of Ni/Mn-NPs

3.5 Atomic force microscopy

Scanning electron microscopy (SEM), one of the most popular techniques for analyzing artificial nanoparticles, was utilized to evaluate the form and appearance of the produced green nanoparticles. The findings indicate that nanoparticles can come in a variety of forms and sizes, proving how extremely varied their morphology can be. The surface of Ni/Mn-NPs has been investigated with a scanning electron microscope (SEM). SEM investigation indicates that the Ni/Mn-NP particles are nanoscale in size and spherical (Figure 3).

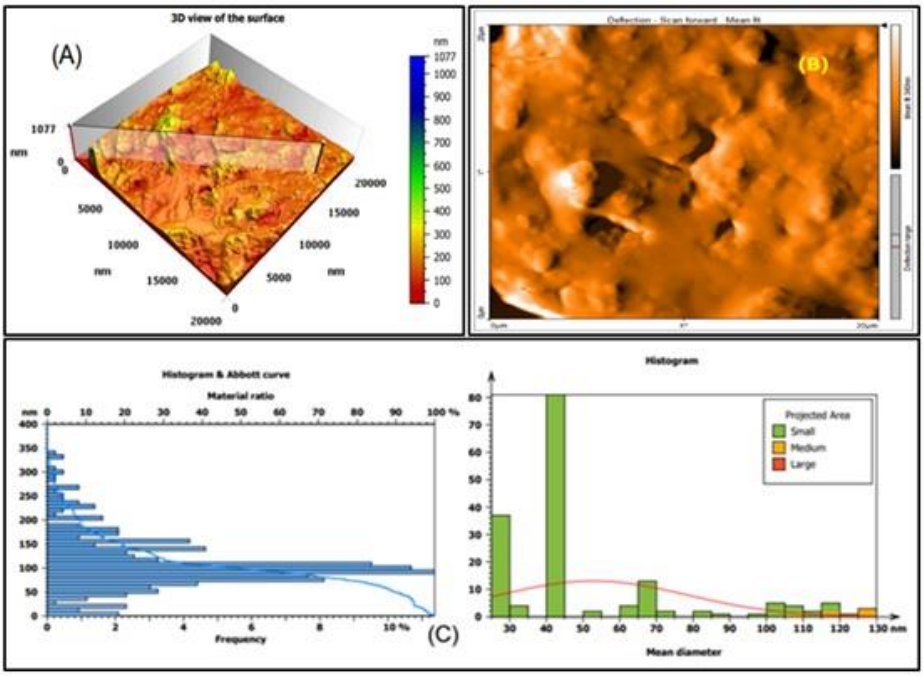

Fig. 4. Atomic force microscopy analysis of Ni/Mn-NPs
(A): 3D of Ni/Mn-NPs, (B): 2D of Ni/Mn-NPs, (C): AFM diagram of the size range of Ni/Mn-NPs.

3.6 X-ray diffractometer

The diffractometer for X-rays (XRD) provides data on phases, mean grain dimension, crystallinity, deformation, and crystalline imperfections furthermore to preferred crystal orientations [24] Figure (5) displays the XRD pattern of Ni/Mn-NPs nanocomposites produced from Lepidium sativum aqueous extracts. The XRD peaks (111), (201), and (080) verified the production of the Ni/Mn nanocomposite. While the weaker peaks, such (220) and (400), match the JCPDS file (No: 47-1049), which shows the cubic system-based crystal structure of NiO, the stronger peaks match the JCPDS file (No: 04-0326), which shows the crystal structure of MnO as an orthorhombic system. Based on the XRD analysis, the generated nanocomposite is composed of cubic NiO and orthorhombic MnO. Using the Debye Scherer Formula, the typical size of a crystallite of Ni/Mn-NPs was calculated from the XRD pattern and found to be 30.87 nm.

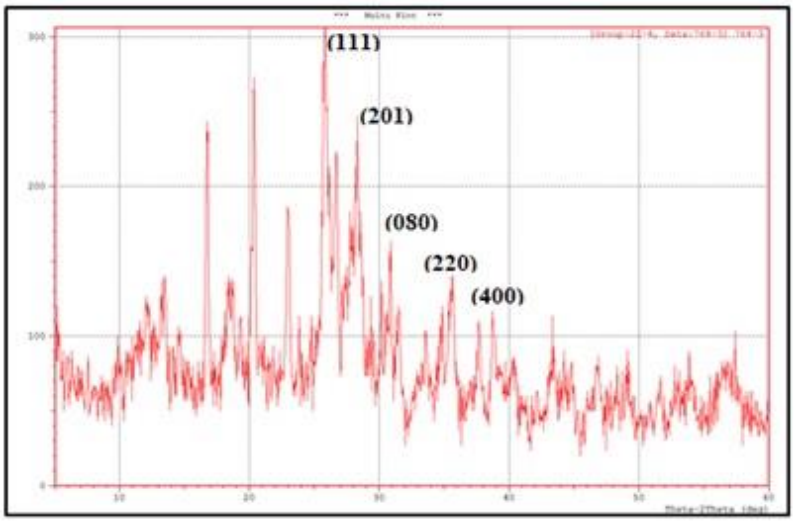

Fig. 5. XRD pattern of Ni/Mn-NPs

3.7 Fourier Transform Infrared (FTIR) Spectroscopy Analysis

The FTIR is the most widely used method for evaluating the presence of particular functional groups in the given nanomaterial [25]. There have been cases where FTIR spectrophotometers have been utilized to acquire spectra with a wavelength as low as 400 cm-1 (25 μm). These spectra had a range that extended from 4000 cm-1 to 670 cm-1, which is equivalent to 2.5 μm to 15 m. Studies conducted on the FTIR spectra of aqueous extracts of Lepidium sativum revealed the presence of a number of functional groups. These groups included C-H stretching, N-H bend, C-C stretching, C-N stretching, and phenolic-OH group stretching. The aldehydic stretching of the C-H and O-H is ascribed to the maxima at around 2941 and 4000–3200 cm–1, respectively [26]. This stretching is analogous to the stretching of alkanes, primary amines, and carboxylic acids [27]. As a result of carbonyl stretching in proteins, the peak that can be found at 1641 cm–1 is (N-H), the presence of aromatic compounds is indicated by the peak 1384 cm-1 corresponding to the C–C stretching bond, while the presence of nitro compounds is demonstrated by the N–O symmetric stretching, (OH) and (C-H, C-O)) were given to the peaks 1109 and 1055, respectively. The existence of the ester may be determined by the presence of the minute peaks at around 1000 cm-1. The peaks with the shortest wavelengths, which are less than 600 cm-1, are indicative of the occurrence of C-Cl stretching in alkyl halides. At peak values of 3369.14, 2921.96, 1608.52, 1404.08, and 1029.92 cm-1, there were noticeable bands of absorbance. The NiO/MnO FTIR Spectra also showed a noticeable absorption band at peak 1101.82 cm-1. Furthermore, the analysis of the samples revealed by FTIR spectroscopy that the Ni/Mn-NPs had notable bands of absorbance at peaks (611.39, 1101.28, 1649.02, and 3369.41) cm -1. The NiO/MnO sample and the Ni/Mn-NPs FTIR Spectra both show a peak (1093.56) that was absent from the Lepidium sativum aqueous extract. As a result, Figure 6 illustrates the production of Ni/Mn-NPs. Metal nanoparticle formation requires a range of compounds derived from plants include, but are not limited to, secondary metabolites that may be found in phenolic acids, proteins, alkaloids, carbohydrates, polyphenols, and terpenoids [22]

The FTIR study demonstrates, that the chlorophyll ester C=O group carries out the role of a reducing agent, and an additional protein is involved in the process of surface capping

of metal nanoparticles which are formed from geranium leaves extract. Thus, the ligands found in plant extracts are responsible for the formation of nanoparticles as well as their stability [25].

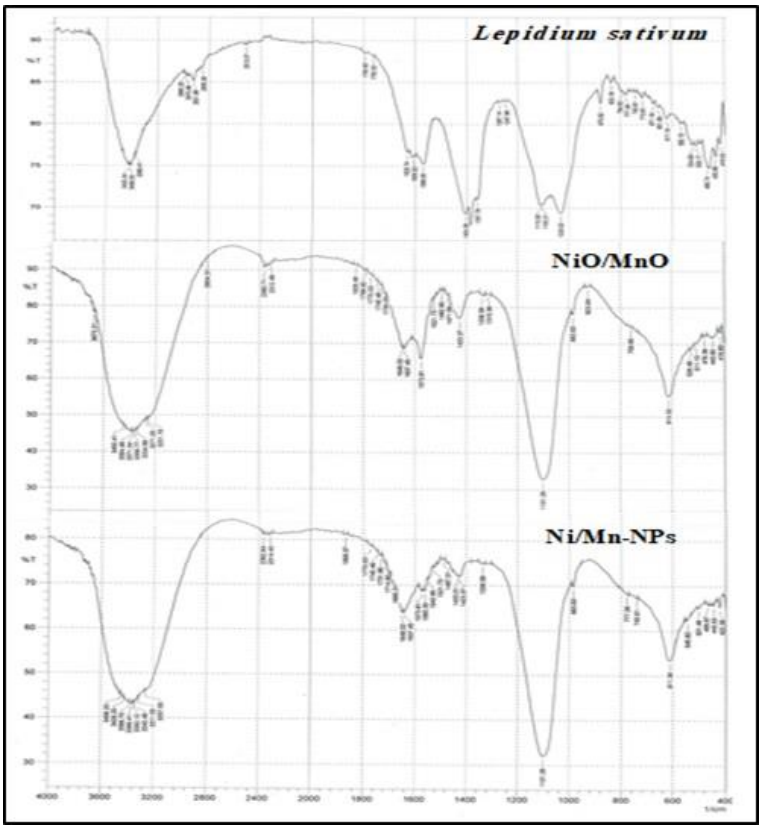

Fig. 6. FTIR Spectra of *Lepidium sativum* aqueous extract, NiO/MnO and Ni/Mn-NPs

3.8 Antibacterial activity of (nickel/manganese-NPs)

3.8.1 Disk diffusion method

The disk-diffusion approach was utilized in order to conduct an examination against S. aureus in order to determine the efficacy of the nanoparticles that were utilized in this study in terms of their antibacterial properties. It was observed that the Ni/Mn-NPs at a concentration of 64 mg/ml demonstrated a higher level of effectiveness compared to those at a concentration of 32 mg/ml. The zone of maximum was determined to be the values of inhibition for (21.67 ± 0.57) mm and (16.33 ± 0.57) mm, respectively, against S. aureus (isolate No. 1), with a statistically significant difference ($P \leq 0.01$), as shown in Tables 3.

Exists a great absence of clearness still on the mechanism of antibacterial effect in metal nanoparticles. Some investigations have been made to clear the antibacterial action. It became well known that some characteristics have a great influence on the antibacterial effectiveness in metal nanoparticles. Such characteristics are size, shape, and surface charge

[20]. Particularly in Gram negative bacteria, nanoparticles may readily penetrate the cell wall of some bacteria and bond with it. After entering the building, they inhibit protein production, deactivate the DNA and enzymes, and ultimately cause the cell of bacteria to die. Additionally, the huge surface dimensions of nanoparticles allow for robust microbial contact [23].

Due to their unique physicochemical characteristics and compact size, Nanoparticles composed of several metals and metal oxides have a great deal of promise for the treatment of a wide variety of diseases and conditions that are caused by drug-resistant bacterial strains. Mult metallic NPs with When compared to mono- and bimetallic NPs, combinations of binary, ternary, and quaternary elements frequently exhibit better chemical, optical, and catalytic qualities. This is due to the fact that different metals complement one another [12]. Bimetallic nanoparticles have been the subject of much investigation during the last 10 years, both as a novel scientific development and as a technical tool to boost productivity. Bimetallic nanoparticles (NPs) have more uses than their corresponding monometallic ones because of the unique catalytic and synergistic capabilities of two separate metals. Depending on their physical and chemical interactions, the spatial overlapping and distribution of two atoms may result in the formation of a core-shell or just an alloy due to the influence of particular metals [21]. As a consequence, Ni/Mn-NPs had a stronger antibacterial effect on the bacteria under investigation than the metals alone because they prevent biofilm formation and accelerate other associated processes, which prevents infections from becoming resistant to them. The antibacterial activity of bimetallic nanoparticles has been evaluated against a range of pathogenic bacteria, with a focus on E. Coli, P. aeruginosa, and S. mutans, which are mostly accountable for human outbreaks. Bimetallic nanoparticles outperform frequently used antibiotics and other antibacterial therapies [14].

Metal ion emission and the production of oxidative stress are the typical descriptions of how nanocomposites kill bacteria, however nonoxidative processes may also function concurrently. Moreover, the generation of ROS disrupts the antioxidant defense mechanism and breaks down the structure of the cell membrane. Additionally, the bulk of recent investigations have established the following nanocomposites action mechanisms: Physical contact-induced cell wall lysis, attachment to microbial cells, ROS production, particle penetration into the cell, oxidative stress-induced protein and DNA damage, and facilitation of internalization. Metal and metal oxide nanocomposites' positively charged surfaces encourage their adherence to bacterial surfaces that are negatively charged, perhaps amplifying their bactericidal activity. Together with it it is also possible that size, Different formulations with different particle sizes and surface charges may affect the NPs' intrinsic properties and alter their capacity to inhibit bacteria [26].

This study agrees with the results of Guo *et al*. [1] who pointed out that due to their diverse antibacterial mechanisms, broad antibacterial range, and outstanding biocompatibility, metal nanoparticles have significant therapeutic use potential.

The main variables that affect a nanoparticle's capacity to fight bacteria include its size, shape, dosage, stability, morphology, and length of treatment [24].

Table 3. Antibacterial activity for Ni/Mn-NPs on(S. *aureus*)isolate

No. of Isolates	**Ni/Mn-NPs**		**LSD Value**
	32mg/ml	**64 mg/ml**	
S_1	16.33± 0.57	21.67 ±0.57	2.170**
S_2	15.67± 0.57	20.67±0.57	2.170**
S_3	12.33±0.57	16.67±0.57	2.170**
S_4	11.33±0.57	15.33±0.57	2.170**

S_5	14.67±0.57	20.33±0.57	2.170**
S_6	15.00±00	20.33±0.57	1.353**
S_7	15.33±0.57	20.33±0.57	2.170**
S_8	15.33±0.57	19.33±0.57	2.170**
S_9	13.33±0.57	16.67±0.57	2.170**
S_{10}	14.67±0.57	20.67±0.57	2.170**
LSD Value	**1.272****	**1.341****	---------
**** (P ≤0.01)**			

3.8.2 (MIC) of the nickel/manganese-NPs

A determination was made on the nanoparticles' minimal inhibitory concentration and its value using a microtiter plate with 96 wells and the process of microdilution using chicken broth. The minimum inhibitory concentration (MIC) of the antibacterial agent against Staphylococcus aureus has been determined using a technique that employs resazurin, which is a colorimetric biomarker of oxidation-oxidation reduction. Resazurin is easily visible to the unaided eye, and spectrophotometer is not necessary to measure the minimum inhibitory concentration (MIC). When oxidized, resazurin is blue; however, when reduced by live cells, it becomes pink [17].
The following were the Ni/Mn-NPs' MIC values when applied to S. aureus isolates: As indicated in Table 4 and Figure 7, was 1 mg/ml in isolates No. 2, 5, 6, 7, and 10, 2 mg/ml in isolates No. 1, 3, 8, and 9, and 4 mg/ml in isolate No. 4.
The findings show that the concentration affected the effectiveness of the Ni/Mn-NPs used in this work, which is consistent with findings from other studies on metal oxide nanoparticles [16]. Additionally, studies show that the size of nanoparticles significantly influences how effective they are against bacteria [19].
Numerous geometries with large surface area, charge, adsorption capacity, and chemical reactivity are present at this nanoscale size, allowing for both severe suppression of biological systems and efficient interaction with them [20].
As a result, we discover that Ni/Mn-NPs' antibacterial activity is significantly influenced by their nanoscale dimensions.

Compromising the integrity of the bacterial membrane provides a good point of attack: interactions between bacterial cell walls and ions from nanoparticles are affected by due to the fact that Both Gram-positive and Gram-negative bacteria have cell walls that are negatively charged but in different proportions [18]. Packirisamy *et al*. [24] *B. subtilis*, *E. coli*, and *P. aeruginosa* were shown to be susceptible to NPs as anti-microbial action, and the sensitivity increased with intensifying one's concentration.

Table 4. MIC of Ni/Mn-NPs on (*S.aureus*) isolate

Isolates	**S1**	**S2**	**S3**	**S4**	**S5**	**S6**	**S7**	**S8**	**S9**	**S10**
Ni/Mn-NPs	2	1	2	4	1	1	1	2	2	1
MIC mg/ml										

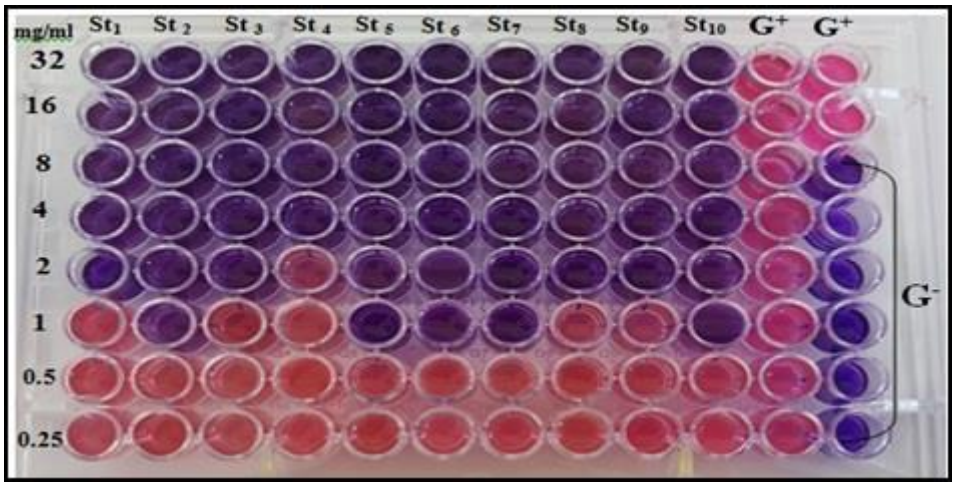

(St): *Staph. aureus* isolate, **(C^+):** Control positive (Bacteria + Media), **(C^-):** Control negative (Media only)

Fig. 7. MIC of Ni/Mn-NPs on *S. aureus* isolate

3.8.3 Anti-Biofilm in Ni/Mn-NPs activity

Biofilms related infections are very frequently hard to control owing to their capability to be highly impervious to treatment [20-25]. That is why, great significance is given to looking for new compounds capable of slowing the bacterial biofilms emergence.

Table 5 shows us the biofilm formation of S. aureus before and after treatment with Ni/Mn-NPs, in 0.5 and 1 $mg.ml^{-1}$ respectively.

Due to the different synergistic interactions between the constituent components, nickel and manganese nanoparticles have a variety of functions and display increased and cumulative capabilities. This study agrees with Basavegowda and Baek [18], pathogenic strains that are both vulnerable to and resistant to antibiotics have been used in tests to determine the antibacterial efficacies of nanoparticles made of metal, metal oxide ions. Among the bacteria E. coli, P. aeruginosa, S. mutans, and S. aureus are only a few examples of the pathogenic bacteria that are the major cause of several infectious disorders. These pathogenic bacteria represent a substantial threat to human health and provide a significant challenge to the healthcare system.

There has been a correlation established between the formation of biofilms and the evolution of germs that are resistant to antibiotic prescriptions [26]. The disappearance of biofilm development following exposure to Ni/Mn-NPs is indicative of the presence of virulence during the process of entering and colonizing host tissue. It was noticed that the growth of biofilm was affected is consistent with the investigations of Cai *et al*. [27], they described the concentration-dependent inhibition of bacterial movement and biofilm formation.

Taking into consideration the findings of the present research, In the near future, more strong antimicrobial drugs may be made using the composites of multimodally nanoparticles

and there to halt the establishment The dissemination of bacterial resistance to traditional antibiotics. Moreover, they could be essential in a number of medicinal applications.

Table 5. Biofilm formation of *S. aureus* before and after treatment with Ni/Mn-NPs.

No. of Isolates	Before Treatment (Control)	After Treatment							
		0.25	**0.5**	**1**	**2**	**4**	**8**	**16**	**32**
S1	Strong	Weak	weak	No Biofilm	No Biofilm	No Biofilm	No Biofilm	No Biofilm	No Biofilm
S2	Strong	Weak	No Biofilm	No Biofilm	No Biofilm	No Biofilm	No Biofilm	No Biofilm	No Biofilm
S3	Strong	Weak	No Biofilm	No Biofilm	No Biofilm	No Biofilm	No Biofilm	No Biofilm	No Biofilm
S4	Strong	No Biofilm	No Biofilm	No Biofilm	No Biofilm	No Biofilm	No Biofilm	No Biofilm	No Biofilm
S5	Strong	Weak	No Biofilm	No Biofilm	No Biofilm	No Biofilm	No Biofilm	No Biofilm	No Biofilm
S6	Strong	Weak	No Biofilm	No Biofilm	No Biofilm	No Biofilm	No Biofilm	No Biofilm	No Biofilm
S7	Strong	Weak	No Biofilm	No Biofilm	No Biofilm	No Biofilm	No Biofilm	No Biofilm	No Biofilm
S8	Strong	Weak	Weak	No Biofilm	No Biofilm	No Biofilm	No Biofilm	No Biofilm	No Biofilm
S9	Moderate	No Biofilm	No Biofilm	No Biofilm	No Biofilm	No Biofilm	No Biofilm	No Biofilm	No Biofilm
S10	Moderate	Weak	No Biofilm	No Biofilm	No Biofilm	No Biofilm	No Biofilm	No Biofilm	No Biofilm

4 Conclusion

In conclusion, the green synthesis technique effectively produces nickel/manganese nanoparticles, and the synthesized Ni/Mn-NPs exhibit substantial ability to kill germs against S. aureus, as well as impede biofilm formation development in S. aureus, contingent upon the concentration employed.

References

1. Guo, Z., Chen, Y., Wang, Y., Jiang, H., and Wang, X. (2020). Advances and challenges in metallic nanomaterial synthesis and antibacterial applications. *Journal of Materials Chemistry B*, **8**(22), 4764-4777. doi: 10.1039/D0TB00099J.
2. Vimbela, G. V., Ngo, S. M., Fraze, C., Yang, L., and Stout, D. A. (2017). Antibacterial properties and toxicity from metallic nanomaterials. *International journal of nanomedicine*, **12**, 3941.doi: 10.2147/IJN.S134526.
3. Almasaudi, S. B. (2018). Acinetobacter spp. as nosocomial pathogens: Epidemiology and resistance features. *Saudi journal of biological sciences*, **25**(3), 586-596. doi: 10.1016/j.sjbs.2016.02.009.
4. Wei, T., Yu, Q., and Chen, H. (2019). Responsive and synergistic antibacterial coatings: fighting against bacteria in a smart and effective way. *Advanced healthcare materials*, **8**(3), 1801381. doi: 10.1002/adhm.201801381.
5. Parthiban, E., Manivannan, N., Ramanibai, R., and Mathivanan, N. (2019). Green synthesis of silver-nanoparticles from Annona reticulata leaves aqueous extract and its mosquito larvicidal and anti-microbial activity on human pathogens. *Biotechnology Reports*, **21**, e00297.
6. Joshi, N. C., and Prakash, Y. A. S. H. W. A. N. I. (2019). Leaves extract-based biogenic synthesis of cupric oxide nanoparticles, characterizations, and antimicrobial activity. *Asian J Pharm Clin Res*, **12**(8), 288-291.
7. Yaqoob, A. A., Parveen, T., Umar, K., and Mohamad Ibrahim, M. N. (2020). Role of nanomaterials in the treatment of wastewater: A review. *Water*, **12**(2), 495. doi: 10.3390/w12020495.
8. Bhumi ,G.; LingaRao, M.and Savithramma N. (2015). Green synthesis of silver nanoparticles from the leaf extract of Adhtoda vasicanees and assessment of its antibacterial activity. Asian J. Pharm. Clin. Res., 8:62–67.
9. Hadjiivanov, K.I.; Panayotov, D.A.; Mihaylov, M.Y.; Ivanova, E.Z.; Chakarova, K.K.; Andonova, S.M. *et al*. (2021). Power of infrared and raman spectroscopies to characterize metal organic frameworks and investigate their interaction with guest molecules. Chemical Review,**121**:1286-1424.
10. Kuppusamy, P., Yusof, M.M., Maniam, G.P. and Govindan, N. (2014). Biosynthesis of metallic nanoparticles using plant derivatives and their new avenues in pharmacological applications—an updated report. *Saudi Pharm. J*. **8**, 473–484.
11. Shankar, S.S., Ahmad, A., Pasricha, R. and Sastry, M. (2003). Bioreduction of chloroaurate ions by geranium leaves and its endophytic fungus yields gold nanoparticles of diferent shapes. *J. Mater. Chem*. **13**, 1822–1826.
12. Mude, N., Ingle, A., Gade, A. and Rai, M. (2009). Synthesis of silver nanoparticles using callus extract of Carica papaya-a frst report. *J. Plant Biochem. Biotechnol*. **18**, 83–86.
13. Dakal, T. C., Kumar, A., Majumdar, R. S., and Yadav, V. (2016). Mechanistic basis of antimicrobial actions of silver nanoparticles, Front. Microbiol. **7** (2016).
14. Vega-Jiménez, A. L., Vázquez-Olmos, A. R., Acosta-Gío, E., and Álvarez-Pérez, M. A. (2019). In vitro antimicrobial activity evaluation of metal oxide nanoparticles. *Nanoemulsions Prop. Fabr. Appl*, 1-18.
15. Zhang, J., Ma, J., Fan, X., Peng, W., Zhang, G., Zhang, F., and Li, Y. (2017). Graphene supported Au-Pd-Fe3O4 alloy trimetallic nanoparticles with peroxidase-like activities as mimic enzyme. *Catalysis Communications*, **89**, 148-151.

16. Godfrey, I. J., Dent, A. J., Parkin, I. P., Maenosono, S., and Sankar, G. (2017). Structure of gold–silver nanoparticles. *The Journal of Physical Chemistry C*, **121**(3), 1957-1963.
17. Arora, N., Thangavelu, K., and Karanikolos, G. N. (2020). Bimetallic nanoparticles for antimicrobial applications. *Frontiers in Chemistry*, **8**, 412.
18. Basavegowda, N., and Baek, K. H. (2021). Multimetallic Nanoparticles as Alternative Antimicrobial Agents: Challenges and Perspectives. *Molecules*, **26**(4), 912.
19. Jesudoss, S. K., Vijaya, J. J., Selvam, N., Kombaiah, K., Sivachidambaram, M., Adinaveen, T. and Kennedy, L. J. (2016). Effects of Ba doping on structural, morphological, optical, and photocatalytic properties of self-assembled ZnO nanospheres. *Clean Technologies and Environmental Policy*, **18**(3), 729-741.
20. Ncube, N. S.; Afolayan, A. J. and Okoh, A. I. (2008). Assessment techniques of antimicrobial properties of natural compounds of plant origin: current methods and future trends. *African Journal of Biotechnology,* **12**(7): 1797-1806.
21. Ogunyemi, S. O., Zhang, F., Abdallah, Y., Zhang, M., Wang, Y., Sun, G. *et al*. (2019). Biosynthesis and characterization of magnesium oxide and manganese dioxide nanoparticles using Matricaria chamomilla L. extract and its inhibitory effect on Acidovorax oryzae strain RS-2. *Artificial cells, nanomedicine, and biotechnology*, **47**(1), 2230-2239.
22. Król, A., Pomastowski, P., Rafińska, K., Railean-Plugaru, V. and Buszewski, B. (2017). Zinc oxide nanoparticles: Synthesis, antiseptic activity and toxicity mechanism. *Advances in colloid and interface science*, **249**, 37-52.
23. Wang, L., Hu, C. and Shao, L. (2017). The antimicrobial activity of nanoparticles: present situation and prospects for the future. *International journal of nanomedicine*, **12**, 1227.
24. Packirisamy, R. G., Govindasamy, C., Sanmugam, A., Karuppasamy, K., Kim, H. S., & Vikraman, D. (2019). Synthesis and antibacterial properties of novel ZnMn2O4–chitosan nanocomposites. *Nanomaterials*, **9**(11), 1589.
25. Kumar, L., Chhibber, S. and K. (2013). Harjai, Zinger one inhibits biofilm formation and improve Antibiofilm efficacy of ciprofloxacin against *Pseudomonas aeruginosa PAO1*. *Fitoterapia*, **90**. 73–78.
26. Rajkumari, J., Busi, S., Vasu, A. C. and Reddy, P. (2017). Facile green synthesis of baicalein fabricated gold nanoparticles and their antibiofilm activity against Pseudomonas aeruginosa PAO1. *Microbial pathogenesis*, **107**, 261-269.
27. Cai, L., Chen, J., Liu, Z., Wang, H., Yang, H. and Ding, W. (2018). Magnesium oxide nanoparticles: effective agricultural antibacterial agent against Ralstonia solanacearum. *Frontiers in microbiology*, **9**, 790.